

PHASES IN AUSTENITIC STAINLESS STEELS

FAZE V AVSTENITNIH NERJAVNIH JEKLIH

Jozef Janovec¹, Borivoj Šuštaršič¹, Jože Medved², Monika Jenko¹

¹ Inštitut za kovinske materiale in tehnologije, Lepi pot 11, 1001 Ljubljana, Slovenija

² Univerza v Ljubljani, NTF-OMM, Aškerčeva 12, 1000 Ljubljana, Slovenija
jozef.janovec@imt.si

Prejem rokopisa – received: 2003-09-03; sprejem za objavo – accepted for publication: 2003-11-20

This study represents a phase characterisation of austenitic stainless steels. A table presents the basic literature data on the phases to be found in austenitic steels. For the as-cast ASTM A351 steel, a thermodynamic prediction and a metallographic identification of phases is also presented. The thermodynamic calculations performed using ThermoCalc revealed austenite, ferrite, $M_{23}C_6$, σ , and Laves as the equilibrium phases at temperatures below 866 K (593 °C). All the predicted phases were also identified experimentally (the Laves phase with some reservation) using a method of selective etching. It was shown that a combination of thermodynamic and metallographic procedures is well suited to phase characterisation in austenitic stainless steels.

Key words: austenitic stainless steels, δ -ferrite, carbides, intermetallic phases, ThermoCalc, phase equilibria, metallography

Prispevek obravnava fazno karakterizacijo avstenitnih nerjavnih jekel in literaturni pregled faz, ki se pojavljajo v tej vrsti jekel. Praktične raziskave so bile opravljene na jeklu vrste ASTM A351 v litem stanju. Delo je bilo usmerjeno v teoretično termodinamično napoved o možni prisotnosti faz in njihovi metalografski identifikaciji pri izbranem jeklu. Za termodinamične izračune je bilo uporabljeno komercialno programsko orodje ThermoCalc. Za termodinamično ravnotežje je bila napovedana prisotnost avstenita, ferita, karbida vrste $M_{23}C_6$ ter σ in Lavesove faze pri temperaturah pod 866 K (593 °C). Vse te faze smo tudi eksperimentalno dokazali v izbranem jeklu z metodami selektivnega jedkanja. Izjema je morda le Lavesova faza, katere prisotnost je delno dvomljiva. V prispevku smo pokazali, da je mogoče s kombinacijo novih modernih računalniško podprtih termodinamičnih orodij in konvencionalnih metalografskih postopkov uspešno izvesti mikrostruktурno karakterizacijo avstenitnih nerjavnih jekel.

Ključne besede: avstenitna nerjavna jekla, δ -ferit, karbidi, intermetalne faze, ThermoCalc, fazna ravnotežja, metalografija

1 INTRODUCTION

Austenitic stainless steels (ASSs) have been used extensively in the food, chemical, and energy industries for nearly one hundred years ^{1,2}. Even if ASSs belong to the group of "more expensive" structural materials, thanks to the considerable amount of alloying elements added, and exhibit some undesirable properties (lower thermal conductivity, higher sensitivity to the stress corrosion cracking and/or intergranular corrosion, lower resistance to the crack formation, etc. ³), they account for about 1.5 % of the world's steel production. The need to achieve high service reliability and safety in nuclear power plants has resulted in extensive investigations of alloy steels, including ASSs. The results of these investigations have been published in many review papers and monographs ^{3,4,6}.

Microstructure stability is one of the most important requirements for assigning the proper mechanical and/or corrosion properties to an ASS. To achieve a stable microstructure, the steels are usually solution heat treated and subsequently annealed at 700–1100 K. During annealing, secondary phases precipitate from the austenite (matrix phase with a f.c.c. crystal lattice) and/or the δ -ferrite (high-temperature phase with a b.c.c. crystal lattice). The most common secondary phases present in advanced ASSs are given in **Table 1** ⁷⁻¹⁶. In

addition to these phases, the orthorhombic M_7C_3 carbide can occur in ASSs with a higher bulk carbon content a mass fraction of 0.3–0.6 % ³. In special ASSs containing higher amounts of silicon or phosphorus, silicides (G-phase with a b.c.c. crystal lattice ³) and phosphides (M_3P with a tetragonal crystal lattice ^{16,17}) were also identified. In some cases, ASSs are used in the as-cast condition (e. g. centrifugally cast or sand-cast large tubes and elbows for pipeline systems). With respect to the highly non-homogeneous microstructure of as-cast steels, information on the portion, the chemical composition, and the stability of the phases (particularly δ -ferrite) is required.

Information about the phases present in ASSs can be obtained experimentally and/or theoretically. Recently, precise experimental techniques for phase identification, such as TEM (including EDX, EELS and electron diffraction ¹⁸⁻²¹), SEM/WDX ^{22,23}, X-ray diffraction ^{24,25}, and DTA ²⁶⁻²⁸ were combined with thermodynamic predictions of phase equilibria and/or the modelling of phase evolution. A similar approach based on a combination of thermodynamic and metallographic procedures was used in this study. The investigation was focused on laboratory-prepared ASTM A351 steel (for the chemical composition, see **Table 2**) in the as-cast condition.

Table 1: The most common secondary phases identified in advanced ASSs. M = metallic part of secondary phase, X = carbon + nitrogen. Concentrations of non-metallic elements are not included.

Tabela 1: Najbolj pogoste sekundarne faze, ki so bile identificirane v razvitih avstenitnih nerjavnih jeklih. M = kovinski del sekundarne faze, X = ogljik + dušik. Niso upoštevane koncentracije nekovinskih elementov.

Phase, crystal lattice	Lattice param. (nm)	Fe (%)	Cr (%)	Ni (%)	Mo (%)	Si (%)	Steel	Ref.
σ -phase, tetrag.	$a = 0.883$ $c = 0.461$	49-52 52 55 19	32-34 38 29 44-48	4-7 5 5 2-6	8-11 — 11 17-19	1 4 — 3	AISI 316 19Cr-12Ni-0.02C AISI 316 20Cr-25Ni-4Mo	7 8 9 10
	$a = 0.475$ $c = 0.779$	37	11	4	42	5-6	AISI 316	7
	$a = 0.473$ $c = 0.772$	38 35	11 13	6 3	45 43-47	— 2	AISI 316 316-LN-3	9 11
	$a = 0.473$ $c = 0.772$							12
χ -phase, b.c.c.	$a = 0.890$ $a = 0.888$	51-53 52 51 48	23-24 21 23 27	4 5 3 3	18 22 21 22	1 — 1 —	AISI 316 AISI 316 316 LN-3 UNS 31803	7 9 13 14
	$a = 1.082$	11-12 9-12 8	29-33 33-48 48	21-26 21-33 37	24-26 24-26 —	6-8 6-9 9	AISI 316 AISI 316A30X 19Cr-12Ni-2Si-0.02C	7 16 8 12
	$a = 1.095$							
	$a = 1.063$ $a = 1.067$ $a = 1.064$ $a = 1.057$	14 17 21-23 17	72 78 62-72 63	3 4 1 2	10 — 1-5 11-13	— — — —	AISI 316 19Cr-12Ni-2Si-0.02C 20Cr-25Ni-4Mo 316LN	15 8 10 13 12
MX, f.c.c.	$a = 0.422$	—	1	—	—	Ti = 99	AISI 321	16
Cr_2N , hexag.	$a = 0.476$ $c = 0.442$	— 1 2-4	100 82 83	— — 2-4	— 4 7-11	— — 1	AISI 316 316 LN-3 20Cr-25Ni-4Mo	7 13 10
	$a = 0.286$ $c = 0.739$	32	43	1	21	1	316 LN-3	13
π -phase, cub. pr.	$a = 0.647$	28 24-26	35 55-58	3 12	30-37 —	— 6-7	UNS 31803 20Cr-25Ni-4Mo	14 10
R-phase, hexag.	$a = 1.093$ $c = 1.934$	32 24	25 23-27	5 5	33-35 46-44	4 5	20Cr-25Ni-4Mo	10

Table 2: Chemical composition of investigated A351 steel. The mass contents of the elements are given in %

Tabela 2: Kemična sestava raziskanega jekla A351. Masni delež elementov (%)

Element	C	Si	Mn	Ni	Cr	Mo	P	S	Fe
Content	0.06	0.43	1.59	11.9	18.0	1.84	0.03	0.01	bal.

Table 3: Phases considered in the thermodynamic calculations

Tabela 3: Faze, upoštevane pri termodinamičnih izračunih

Group of phases	Phase
Basic (polymorphous) phases	liquid, f.c.c. (austenite), b.c.c. (α - and/or δ -ferrite)
Carbides	M_3C , M_7C_3 , M_{23}C_6 , M_6C
Intermetallic phases	Laves, χ (chi), σ (sigma)

2 METHODS AND RESULTS

2.1 Thermodynamic calculations

The thermodynamic calculations were performed with the ThermoCalc program²⁹ using the database for iron-based systems formulated by Kroupa et al.³⁰. Sulphur and phosphorus were not considered in the calculations because they are not included in the database. In this study:

Phase equilibria for the Fe-(16-24)Cr-0.06C-0.43Si-1.59Mn-11.9Ni-1.84Mo system were calculated in the temperature range 400-1800 K and the results achieved were presented in the form of a vertical section of the phase diagram, **Figure 1**.

Volume fractions of polymorphous equilibrium phases were predicted for the Fe-18Cr-0.06C-0.43Si-1.59Mn-11.9Ni-1.84Mo system in the temperature range 500-1694 K, **Figure 2**.

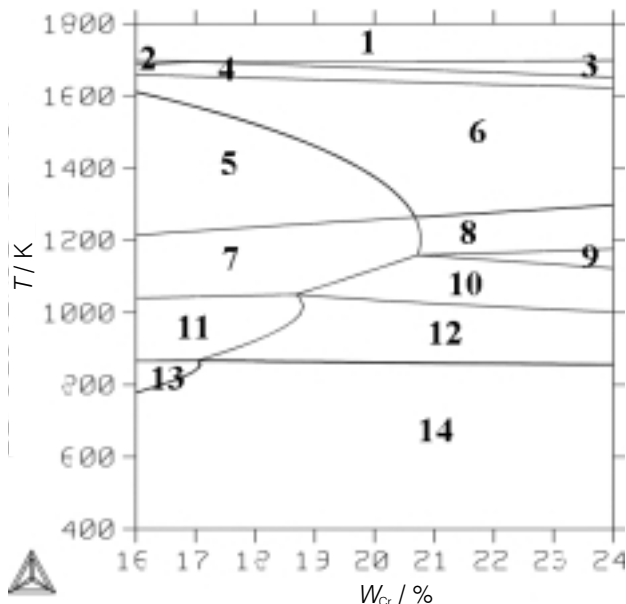


Figure 1: Vertical section of the phase diagram predicted for Fe-(16-24)Cr-0.06C-0.43Si-1.59Mn-11.9Ni-1.84Mo system. Individual phase equilibria are marked with numbers:

1	liquid	8	f.c.c.+b.c.c.+M ₂₃ C ₆
2	liquid+f.c.c.	9	f.c.c.+b.c.c.+M ₂₃ C ₆ +σ
3	liquid+b.c.c.	10	f.c.c.+M ₂₃ C ₆ +σ
4	liquid+f.c.c.+b.c.c.	11	f.c.c.+M ₂₃ C ₆ +Laves
5	f.c.c.	12	f.c.c.+M ₂₃ C ₆ +σ+Laves
6	f.c.c.+b.c.c.	13	f.c.c.+b.c.c.+M ₂₃ C ₆ +Laves
7	f.c.c.+M ₂₃ C ₆	14	f.c.c.+b.c.c.+M ₂₃ C ₆ +σ+Laves.

Slika 1: Vertikalni prerez za napovedan fazni diagram Fe-(16-24)Cr-0.06C-0.43Si-1.59Mn-11.9Ni-1.84Mo. Posamična fazna ravnotežja so označena s številkami:

1	talina	8	p.c.k.+t.c.k.+M ₂₃ C ₆
2	talina+p.c.k.	9	p.c.k.+t.c.k.+M ₂₃ C ₆ +σ
3	talina+t.c.k.	10	p.c.k.+M ₂₃ C ₆ +σ
4	talina+p.c.k.+t.c.k.	11	p.c.k.+M ₂₃ C ₆ +Laves
5	p.c.k.	12	p.c.k.+M ₂₃ C ₆ +σ+Laves
6	p.c.k.+t.c.k.	13	p.c.k.+t.c.k.+M ₂₃ C ₆ +Laves
7	p.c.k.+ M ₂₃ C ₆	14	p.c.k.+t.c.k.+M ₂₃ C ₆ +σ+Laves.

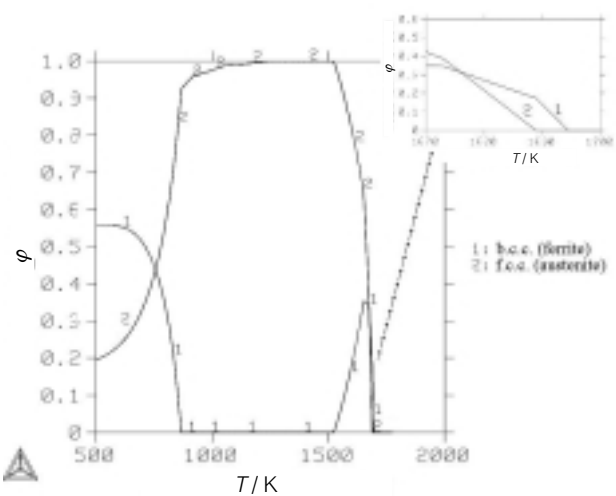


Figure 2: Calculated volume fractions of b.c.c. and f.c.c. phases, with the dependence on temperature. Small diagram in the upper-right corner indicates changes in volume fraction of the phases at the temperatures of the solid \leftrightarrow liquid transition.

Slika 2: Izračunana delež faz t.c.k. in p.c.k. v odvisnosti od temperature. Manjši diagram v zgornjem desnem kotu prikazuje spremembe v volumenskem deležu faz pri temperaturi prehoda trdno \leftrightarrow talina.

The phases considered in the thermodynamic calculations are given in **Table 3**. In the vertical section of the phase diagram (Figure 1), fourteen areas corresponding to the one- (marked with 1, 5), two- (2, 3, 6, 7), three- (4, 8, 10, 11), four- (9, 12, 13), or five-phase (14) equilibria are illustrated. The five-phase equilibrium consisting of f.c.c., b.c.c., M₂₃C₆, σ, and Laves appears at temperatures below 866 K. The calculated volume fractions of b.c.c. and f.c.c. polymorphous phases are documented, with their dependence on temperature, in **Figure 2**. The larger window for the extend temperature range was completed with a smaller one showing changes in the volume fractions of the above-mentioned

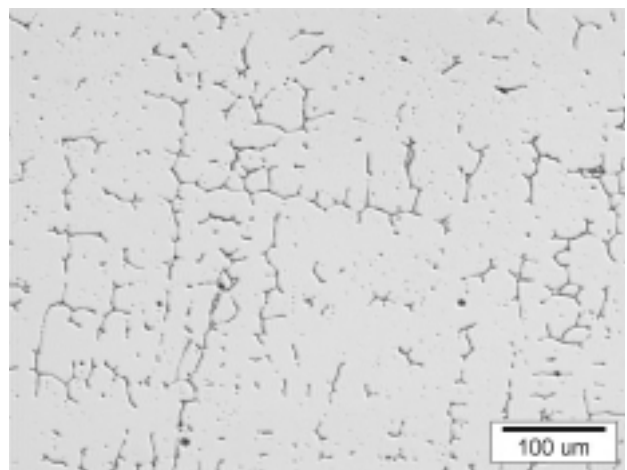


Figure 3: Microstructure of the steel after etching in agent A. The background is formed by austenite; the dark longitudinal areas are formed by δ-ferrite.

Slika 3: Mikrostruktura jekla po jedkanju v raztopini A. Matica je avstenit, temeljne podolžne površine so δ-ferit.

phases at temperatures of 1670–1700 K (solid \leftrightarrow liquid transition).

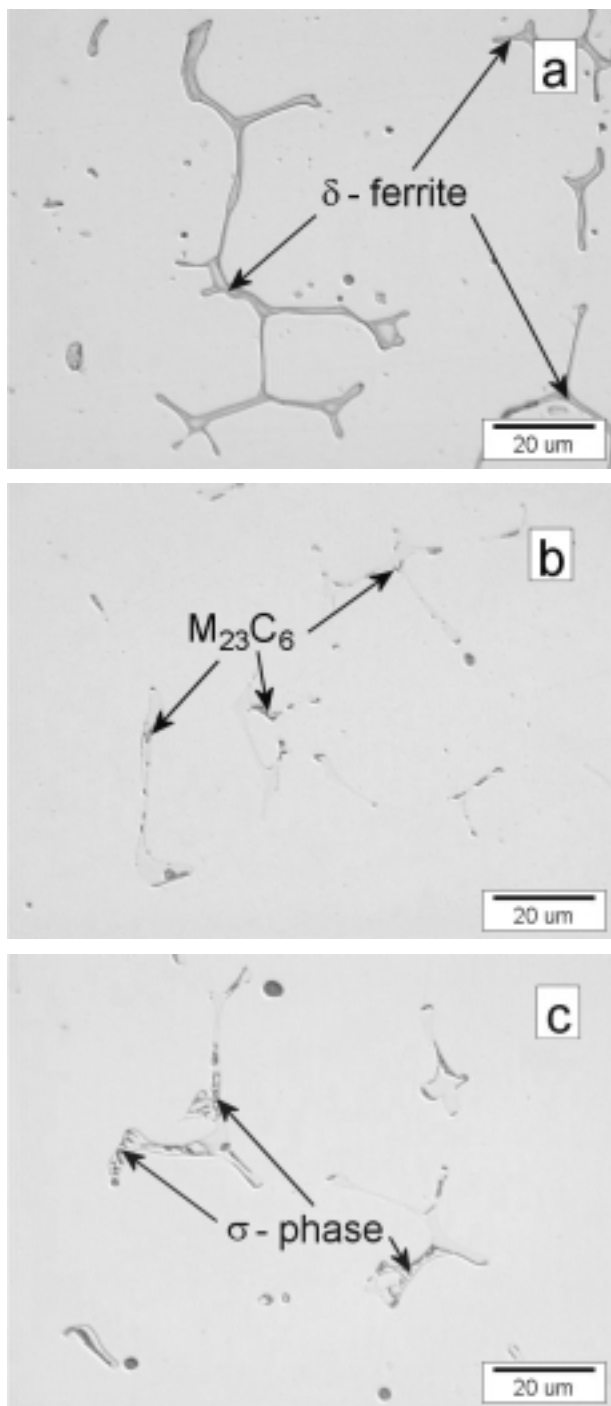


Figure 4: Different phases identified in the microstructure of the steel by selective etching:

- a) δ-ferrite, etched in agent A,
- b) M₂₃C₆ carbide, etched in agent B (Groesbeck),
- c) σ-phase, etched in agent C (Glyceregia).

Slika 4: Različne faze, identificirane v mikrostrukturi jekla s selektivnim jedkanjem:

- a) δ-ferit, jedkano z raztopino A
- b) karbid M₂₃C₆, jedkano z raztopino B (Groesbeck)
- c) σ-faza, jedkano z raztopino C (glicerinska zlatotopka)

2.2 Metallographic observations

For the experimental identification of the thermodynamically predicted phases, a metallographic method of selected etching was applied. The agents (A, B, and C) used in the etching of the metallographic sample are characterised in **Table 4**^{31,32}. To distinguish between δ-ferrite and austenite, the etching agent A was used, **Figures 3 and 4a**. The experimentally determined volume fraction of δ-ferrite is about 2 %. At the boundaries between the austenite matrix and the islands of δ-ferrite, longitudinal particles of the M₂₃C₆ carbide were revealed by etching in agent B, **Figure 4b**. Etching in agent C revealed nets of σ-phase and discrete particles with a mottled appearance in the interior of the δ-ferrite, **Figure 4c and 5**.

3 DISCUSSION

3.1 The volume fraction of δ-ferrite

The volume fraction of δ-ferrite is an important parameter that influences the microstructure stability and the properties of dual-phase steels. This parameter was also evaluated in this study because the formation of δ-ferrite in the investigated steel was expected.

The thermodynamic calculations revealed a stable δ-ferrite in the temperature range 1522–1694 K, **Figures 1 and 2**. The highest volume fraction of this phase (about 35 %) was predicted for temperatures between 1650 K and 1673 K, where the three-phase equilibrium (liquid + f.c.c. + b.c.c.) exists. The disappearance of a liquid phase from the equilibrium (below 1650 K) results in a drastic decrease in the volume fraction of δ-ferrite. The above theoretical considerations indicate that a

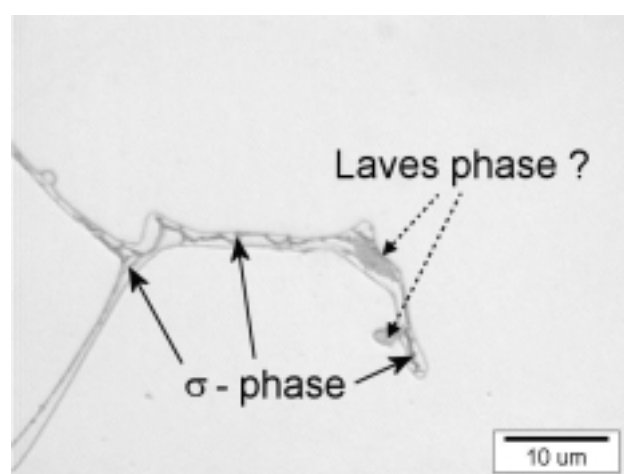


Figure 5: Microstructure of the steel after etching in agent C (Glyceregia). Inside of δ-phase areas, σ-phase nets and discrete particles of mottled appearance (probably Laves phase) are present.

Slika 5: Mikrostruktura jekla po jedkanju v raztopini C (glicerinska zlatotopka). V notranjosti δ-faze je mreža σ-faze in diskretna zrna sive barve (verjetno Lavesova faza).

Table 4: Agents used in the selective etching of phases
Tabela 4: Raztopine, uporabljene za selektivno jedkanje

Symbol	Mark	Chemical composition	Effect	Reference
A	–	30 g KOH + 30 g K ₃ [Fe(CN) ₆] + 60 g H ₂ O	Selective etching of δ-ferrite.	³¹
B	Groesbeck	4 g KMnO ₄ + 4 g NaOH + 100 ml H ₂ O	Selective etching of carbides.	³¹
C	Glyceregia	10 ml HNO ₃ + 35 ml HCl + 30 ml glycerol	Selective etching of σ-phase.	³²

larger volume fraction of δ-ferrite can be achieved in two ways:

- By slow cooling in the temperature range 1650–1673 K, which brings the steel close to equilibrium. At this point the volume fraction of δ-ferrite in the steel should be comparable with the equilibrium level (about 35%).
- By changing the steel's chemical composition in terms of an increase in the bulk content of ferrite-stabilising elements. It is generally known that the ferrite-stabilising elements extend the area of the δ-ferrite's stable existence and the austenite-stabilising elements act against this tendency.

A comparison of the experimental (about 2 %) and predicted (35 %) values indicate that the cooling rate in the temperature range 1522–1694 K was too high to bring the investigated steel close to equilibrium during casting and to enhance in this way the volume fraction of δ-ferrite.

3.2 The occurrence of carbides

Three types of carbides (M₇C₃, M₂₃C₆, and M₆C) would be expected in the as-cast microstructure of the investigated steel. However, the lower bulk carbon content (and consequently the higher Cr/C ratio) and the lower molybdenum content strongly restrict the precipitation of M₇C₃ and M₆C carbides ^{6,33}, respectively. Thus, the longitudinal particles observed along the ferrite/austenite boundaries, Figure 4b, can be identified as M₂₃C₆ carbide, regardless of the ability of agent B to etch other alloy carbides ³¹.

M₂₃C₆ particles were observed to precipitate preferentially along ferrite/austenite interfaces. The reason is due to the differences in the chemical compositions of the above polymorphous phases. In austenite and ferrite it is austenite- (C, Ni, Mn) and ferrite-stabilising elements (Cr, Mo, Si), respectively, that tend to dominate ^{34,35}. For precipitation of the M₂₃C₆ carbide, carbon and chromium are mainly required. The ferrite/austenite interface attracts carbon from austenite and chromium from ferrite, so it is the most convenient location for the M₂₃C₆

precipitation. M₂₃C₆ precipitation at the ferrite/austenite interface was also observed in the 12 % Cr steel ³⁶.

3.3 The occurrence of intermetallic phases

Laves and σ are typical phases in low-carbon ASSs ³⁷. They were predicted to appear at temperatures below 1048 K (Laves) and 922 K (σ) in the investigated steel. The prediction was also confirmed by metallographic observations. The σ phase was identified in the microstructure of the investigated steel unambiguously, by means of the etching agent C. Particles of this phase were found to form nets in the interior of the δ-ferrite, **Figures 4c and 5**. In the same microstructure, particles of mottled appearance, strongly resembling a Laves phase ³⁸, were observed. However, this cannot be considered as metallographic evidence for the phase.

3.4 Methodological remarks

In this study, good agreement between the results of the thermodynamic calculations and the metallographic observations (selective etching, light microscopy) was achieved. In general, light microscopy is considered as a less precise tool for microstructure characterisation. However, if methods of light microscopy are combined with sufficiently correct thermodynamic predictions, reliable results can be obtained.

4 CONCLUSIONS

Aspects of this study can be characterised in both scientific and methodological areas. From the scientific point of view, five phases (f.c.c., b.c.c., M₂₃C₆, σ, and Laves) were thermodynamically predicted to occur in the as-cast ASTM A351 steel. Four of these phases were also identified experimentally with metallographic procedures (selective etching, light microscopy). The Laves phase was identified, but with some reservations. A new procedure was proposed (thermodynamic calculations + metallographic observations) for the prediction of the δ-phase volume fraction in as-cast ASSs. In addition, the less-exact procedure of light microscopy

can reveal sufficiently reliable results if it is combined with sufficiently correct thermodynamic predictions.

ACKNOWLEDGEMENT

The authors acknowledged the support of the Slovenian Ministry of Education, Science and Sport under grant No. L2-3094-0206-02/IMT. They also wish to thank Bojan Breskvar for the alloy preparation as well as Dr. Matjaž Godec and Nataša Lipovšek for their assistance with the metallographic observations.

5 REFERENCES

- ¹ B. Strauss, E. Maurer, Kruppsche Monatsh., 1 (**1920**) 120
- ² E. C. Bain, W. E. Griffiths, Trans. Am. Inst. Mining Met. Eng., 75 (**1927**) 166
- ³ A. F. Padilha, P. R. Rios, ISIJ Int., 42 (**2002**) 325
- ⁴ C. J. Novak, Handbook of Stainless Steels, eds. D. Peckner, I. M. Bernstein, McGraw Hill, New York 1976
- ⁵ P. Marshall, Austenitic Stainless Steels, Elsevier Applied Science Publishers LTD, London 1984
- ⁶ J. Janovec, Nature of Alloy Steel Intergranular Embrittlement, VEDA, Bratislava 1999
- ⁷ M. Vodárek, M. Sobotková, J. Sobotka, Kovové Mater., 27 (**1989**) 23
- ⁸ M. Vodárek, J. Sobotka, M. Sobotková, Z. Metallkde., 82 (**1991**) 22
- ⁹ B. Weiss, R. Stickler, Metall. Trans., 3A (**1972**) 851
- ¹⁰ R. F. A. Jagelius-Petterson, Scripta Metall. Mater., 28 (**1993**) 1399
- ¹¹ J. K. L. Lai, D. J. Chastell, P. E. J. Flewitt, Mater. Sci. Engn., 49 (**1981**) 19
- ¹² L. P. Stoter, J. Metal Sci., 16 (**1981**) 1039
- ¹³ R. A. Mulford, E. L. Hall, C. L. Briant, Corrosion, 39 (**1983**) 132
- ¹⁴ J. O. Nilson, P. Liu, Mater. Sci. Technol., 7 (**1991**) 853
- ¹⁵ M. Vodárek, J. Sobotka, M. Sobotková, Kovové Mater., 26 (**1988**) 649
- ¹⁶ P. Záhumenský, S. Tuleja, J. Országhová, J. Janovec, V. Magula, Corrosion, 57 (**2001**) 874
- ¹⁷ P. Ševc, D. Mandrino, J. Blach, M. Jenko, J. Janovec, Kovové Mater., 40 (**2002**) 35
- ¹⁸ M. Prikryl, A. Kroupa, G. C. Weatherly, S.V. Subramanian, Metall. Mater. Trans., 27A (**1996**) 1149
- ¹⁹ A. Výrostková, A. Kroupa, J. Janovec, M. Svoboda, Acta Mater., 46 (**1998**) 31
- ²⁰ A. Kroupa, A. Výrostková, M. Svoboda, J. Janovec, Acta Mater., 46 (**1998**) 39
- ²¹ V. Homolová, J. Janovec and A. Kroupa, Mater. Sci. Eng., 335A (**2002**) 279
- ²² J. Sopoušek, J. Vřeš ál, Z. Metallkde, 85 (**1994**) 111
- ²³ J. Sopoušek, J. Vřeš ál, Z. Metallkde, 85 (**1994**) 116
- ²⁴ C. Allibert, C. Bernerd, M. Valignat, M. Dombre, J. Less Common Mater., 59 (**1978**) 211
- ²⁵ A. Kusoffsky, B. Jansson, Calphad, 21 (**1997**) 321
- ²⁶ B. J. Lee, Metall. Trans., 24A (**1993**) 1017
- ²⁷ Y. Du, J. C. Schuster, Metall. Mater. Trans., 30A (**1999**) 2409
- ²⁸ V. Homolová, J. Janovec, M. Kusý, R. Moravčík, E. Illeková, P. Grgač, Can. Metall. Quart., 42 (**2003**) 89
- ²⁹ J. O. Andersson, T. Helander, L. Höglund, P. Shi, B. Sundman, Calphad, 26 (**2002**) 273
- ³⁰ A. Kroupa, J. Havránková, M. Coufalová, M. Svoboda, J. Vřeš ál, J. Phase Equi., 22 (**2001**) 312
- ³¹ G. Petzow, Metallographic etching, ASM, Ohio 1978
- ³² R. F. Mehl, Metals Handbook, Atlas of Microstructures of Industrial Alloys, ASM, Ohio 1972
- ³³ R. W. K. Honeycombe, Structure and Strength of Alloy Steels, Climax Molybdenum Co., 1973
- ³⁴ A. Kroupa, L. Karmazin, M. Svoboda, Mater. Sci. Engn, A127 (**1990**) L11
- ³⁵ M. Svoboda, A. Kroupa, L. Karmazin, Mater. Sci. Technol., 10 (**1994**) 691
- ³⁶ J. Janovec, M. Svoboda, J. Blach, Mater. Sci. Engn., A249 (**1998**) 184
- ³⁷ V. Homolová, P. Záhumenský, A. Kroupa, Kovové Mater., 38 (**2000**) 365
- ³⁸ J. Janovec, B. Richarz, H. J. Grabke, Scripta Metall. Mater., 33 (**1995**) 295